Chemical Engineering Journal 158 (2010) 384–392

Contents lists available at ScienceDirect

Chemical Engineering Journal

journal homepage: www.elsevier.com/locate/cej

Experimental kinetic analysis of ethylene absorption in ionic liquid [Bmim]NO_3 with dissolved $AgNO_3$ by a semi-continuous process

H.R. Mortaheb*, M. Mafi, B. Mokhtarani, A. Sharifi, M. Mirzaei, N. Khodapanah, F. Ghaemmaghami

Chemistry and Chemical Engineering Research Center of Iran, Tehran, P.O. Box: 14335-186, Iran

ARTICLE INFO

Article history:
Received 16 August 2009
Received in revised form 2 January 2010
Accepted 4 January 2010

Keywords:
Ionic liquid
Ethylene absorption
Silver nitrate
Semi-continuous system
Gaseous mixture

ABSTRACT

The ability of silver ions to form reversible π-bond complexation with unsaturated hydrocarbons can be utilized to separate olefins from paraffins using a solution of $AgNO_3$ dissolved in an ionic liquid (IL). The process is suggested because of zero vapor pressure of the solvent, which results in higher purity of the separated product in comparison to when an aqueous $AgNO_3$ solution is applied. In the present study, 1-butyl-3-methylimidazolium nitrate ([Bmim]NO_3), an IL that can dissolve $AgNO_3$, is applied as the solvent. The absorption of ethylene from a gaseous mixture of ethylene/ethane with constant flowrate in the silver nitrate dissolved media is investigated in silver nitrate concentrations of 1, 2 and 5 M, and temperatures within the range of 5–35 °C. The absolute absorptivity of ethylene is increased from 1.12 to 5.68 g l^{-1} at 25 °C when the concentration of $AgNO_3$ is increased from 1 to 5 M. Maximum absorption of ethylene is found at near ambient temperatures (15 °C). The absorption selectivity of ethylene to ethane increases with increase of $AgNO_3$ concentration and decrease with increasing temperature. The capacity of ethylene absorption in the reactive media at 25 °C and 5 M concentration of $AgNO_3$ is about 0.43 of that for the aqueous $AgNO_3$ solution. The results of an applied theoretical model for prediction of total ethylene absorption can be verified by the experimental results.

1. Introduction

Large amounts of olefin/paraffin gaseous mixtures are produced in the refineries by the processes such as Fischer–Tropsch synthesis, ethane cracking, and also from dehydrogenation unit [1,2]. Low-temperature distillation is a classical method for separation of olefins from light gases [3,4] that requires large number of stages and/or high reflux ratios [1]. Extractive distillation, as an alternative separation method [3,4], requires additive reagents for enhancing relative volatility of paraffins to olefins [5]. Physical adsorption by applying ion exchange molecular sieves such as zeolites can also be used for separation of a gaseous mixture species. These methods are expensive, appropriate for feeds with high fractions of olefins, and consume large amount of energy [3]. On the other hand, chemical absorption of olefins by metallic ions such as silver and copper can be applied promisingly for separation of such gaseous mixtures, as those ions have no tendency to absorb paraffins [4,6–11]. Silver ions can bind specifically and reversibly with olefins. This complexation reaction is reversible with temperature and/or pressure changes. Olefin molecules donate π electrons from their occupied 2p orbitals to the empty s orbitals of the silver ions to form σ-bonds. Back donation of electrons from the occupied d orbitals of the silver ions into the empty π*–2p antibonding orbitals of the olefin molecules results in π-bonding. Therefore, silver ions can act as olefin carriers [10,12].

Some processes for separation based on chemical absorption in an aqueous solution supported on solid substrates [13,14] have been far proposed [1]. However, due to relatively high vapor pressure of water as the solvent, using a further step for removal of water to purify the product is inevitable. On the other hand, increasing temperature or applying a sweep gas in the regeneration step also causes more evaporation of the solvent [1]. Therefore, applying a solvent with negligible vapor pressure, such as an ionic liquid, may resolve the problem.

Ionic liquids are salts with an organic cation and monovalent inorganic anions. These materials have low melting points (generally less than 253 K), and high thermal resistance, and are liquid in a wide range of temperature. Properties of ionic liquids mainly depend on the characteristics of their anions. These materials are strong ionization reagents but have low dielectric constants [1,15]. They have been used increasingly as "green solvents" in recent years due to their low vapor pressure, nonflammability, low poisoning, and ease of recovery. Most of recent researches consider the application of ionic liquids in catalytic reactions, organic synthesis, and electrochemistry. Some studies have been done by applying ionic liquids in separation of olefins/paraffins in recent years. One of these works studies the solubility of metallic salts in ionic liquids and also absorption of 1-buthene and

* Corresponding author. Tel.: +98 21 44580751; fax: +98 21 44580781.
E-mail address: mortaheb@ccerci.ac.ir (H.R. Mortaheb).

1385-8947/$ – see front matter © 2010 Elsevier B.V. All rights reserved.
doi:10.1016/j.cej.2010.01.001

Nomenclature

a/cm^{-1} interfacial area
C_A/mol cm^{-3} ethylene concentration
$C_{A,b}$/mol cm^{-3} ethylene concentration (in bulk phase)
C_A^*/mol cm^{-3} ethylene solubility
C_B^{bulk}/mol m^{-3} silver nitrate concentration
d/cm bubble diameter
d_{pa}/cm diameter of parabola-shaped bubble
D_A/cm^2 s^{-1} diffusivity
E/dimensionless enhancement factor
f/cm minor axis of the projected ellipsoid
F/cm major axis of the projected ellipsoid
h/cm liquid level in absorption column after bubbling
h_0/cm liquid level in absorption column before bubbling
h_{pa}/cm height of parabola-shaped bubble
H/bar cm^3 mol^{-1} Henry's constant
Ha/dimensionless Hatta number
k/m^3 mol^{-1} s^{-1} rate constant
k_L, k_g/cm s^{-1} liquid-side and gas-side mass transfer coefficients
k_{ov}/s^{-1} overall reaction rate constant
N/mol cm^{-3} s^{-1} absorption rate ($=N_A \times a$)
N_A/mol cm^{-2} s^{-1} absorption flux
P_A/bar ethylene partial pressure
Q/cm^3 min^{-1} volume flowrate of gas mixture
r/mol m^{-3} s^{-1} reaction rate
R/J mol^{-1} K^{-1} universal gas constant (8.314 J mol^{-1} K^{-1})
t/min elapsed absorption time
t_b/s time to traverse one bubble diameter
T/K absolute temperature
v_A/l mol^{-1} gas molar volume at the normal boiling point
x/dimensionless mass fraction of ethylene

Greek letters
ε gas hold-up (dimensionless)
μ_{IL}/cP ionic liquid viscosity
ρ/g cm^{-3} density of gas mixture

Subscripts
in inlet flow to the absorption column
out outlet flow from the absorption column

butane in several ionic liquids including silver and copper salts [1]. Kang et al. [10] studied the separation of isoprene/*n*-pentane mixtures through the use of facilitated transport membranes containing complexes of silver ions with an ionic liquid 1-butyl-3 methyl imidazolium tetrafluoroborate ([Bmim]BF_4). In another study, they investigated the effect of three different ionic liquids on the formation of a partial positive charge on the surface of silver nanoparticles and its subsequent effect on the facilitated olefin transport. [Bmim]BF_4/Ag membrane showed the best performance for separation of propylene/propane among the three membranes [16]. Kang et al. [17] also observed that among the three ionic liquids of [Bmim]X (X = BF_4, NO_3, CF_3SO_3) in poly(2-ethyl-2-oxazoline)/$AgNO_3$ facilitated membranes, [Bmim]NO_3 has the most improved performance for separation of propylene/propane mixture. Ortiz et al. [18] studied the selective absorption of propylene from the mixture with propane by chemical complexation with silver ions in [Bmim]BF_4/$AgBF_4$ solution. Their study has shown that the sorption capacity of the olefin via silver complexation in ionic liquid media is even more than that in the corresponding aqueous solution. Huang et al. [19] reported an immobilized liquid membrane system for separation of olefins and paraffins (1-pentene/pentane) based on a new class of silver containing ILs.

While the absorption of olefins in $AgNO_3$ solutions were often measured in batch systems [8,11], Chang et al. [20] developed a continuous isothermal separation process for propylene/propane mixture using $AgNO_3$ solution and zirconium oxide membrane. In similar studies, facilitated transport membranes were applied to ethylene/ethane separation using silver nitrate as the carrier [21,22].

Although the above-mentioned studies have shown that using ionic liquids in olefin/paraffin separations is a promising application, more researches are still required in this field. In the present study, absorption of ethylene from an ethylene-ethane mixture in a solution of $AgNO_3$ in 1-butyl-3-methylimidazolium nitrate ([Bmim]NO_3) is studied. A semi-continuous setup is applied for the present study, which resembles more to the industrial absorption systems.

2. Materials and equipment

2.1. Materials

The following materials were purchased from manufacturers and used without further treatments in this study.

$AgNO_3$; 99.9% (Merck), ethylene; 99.5% (Air Products), ethane; 99.5% (Air Products), nitrogen; 99.5% (domestic manufacture), NMP; 99.5% (Merck); 1-chloro butane; 99% (Merck), 1-methyl imidazole; 99% (Merck), P_2O_5; 97% (Merck), dichloromethane; 99% (Merck); $NaNO_3$; 99.5% (Fluka), acetonitrile; 99% (Merck), ethyl acetate; 99.5% (Merck), Alumina; 100–120 mesh (Fluka), and silica gel; 60 mesh (Fluka). Double distilled water used in the experiments was prepared in the laboratory (electrical conductivity = 4.9 μs cm^{-1}).

[Bmim]NO_3 is prepared in our laboratory through the following procedure: In order to synthesis [Bmim]NO_3, [Bmim]Cl is first synthesized following the procedure in literature [23]. 51 g (0.6 mol) of $NaNO_3$ is added to 87.32 g (0.5 mol) of [Bmim]Cl, which is dissolved in dichloromethane and stirs for 24 h at room temperature. The produced suspension is filtered for removal of NaCl and it is washed several times with small volume of water until no further AgCl is precipitated by adding $AgNO_3$. The solvent is evaporated under vacuum and the ionic liquid is mixed by activated charcoal for 12 h. The procedure results in 42.43 g of [Bmim]NO_3 with 72% yield [24]. The NMR of synthesized ionic liquid is as follows:

^{1}H NMR (500 MHz; D_2O): 0.86 (3H, t, J = 7.4), 1.27 (2H, m), 1.80 (2H, m), 3.88 (3H, s), 4.16 (2H, t, J = 7.2), 7.43 (1H, t, J = 1.7), 7.47 (1H, t, J = 1.7), 8.71 (1H, s)

The water content of the synthesized ionic liquid by Karl Fischer is measured to be less than 5 ppm.

2.2. Equipment

The flow rates of gases are measured by an intelligent digital flowmeter (1000-series, Varian) and calibrated rotameters (Cole Parmer) in the room temperature and pressure. The rotameters uncertainties amount up to about ±0.5%. A water bath (Huber, Polystat cc1) is used to control the temperature of absorption column. The concentration of ethane, ethylene, and nitrogen gas in the inlet and outlet are measured by a gas chromatograph, GC, with an auto injector (3800, Varian). The GC uncertainty is determined up to about ±0.45%. The applied detector is TCD and the type of column is 2 m × 6.3 mm × 4 mm PORAPAK. Helium is used as carrier gas in the GC. A digital manometer is used to measure the pressure of the column.

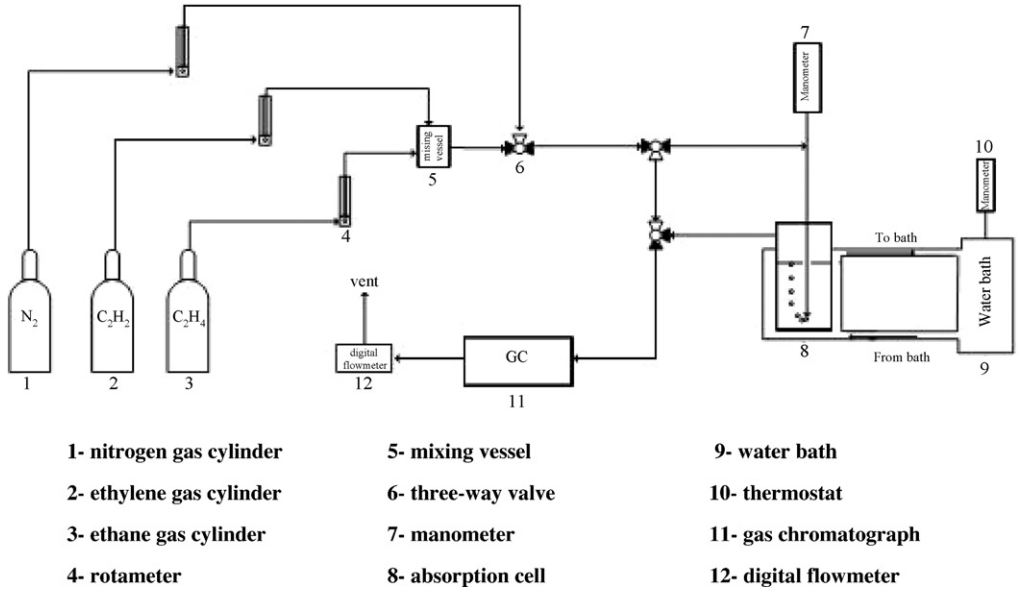

Fig. 1. Schematic diagram of setup in the experiments. Solid triangles in the valves show the direction of flow in the absorption mode.

3. Experimental method

The experimental setup is presented in Fig. 1. Ethane and ethylene are mixed in a mixing vessel. The setup is equipped with 3-three way valves. The initial concentration and flowrate of influent mixture can be measured by changing the direction of flow in the valves so that the absorption column is located in the bypass way and the feed gas is entered directly to the GC and then to the digital flowmeter. The influent gas with volumetric ethane/ethylene ratio of 1:1 and flowrate of 60 ml min^{-1} enters to a 20-ml absorption column through a sinter-glass distributor located at the bottom of absorption column. Gas bubbles are absorbed in the liquid during rising in the absorption column. The unabsorbed gas exits from the top of the column, is introduced to the GC and then to the digital flowmeter. The absorption column is placed in the water bath to control the temperature. The temperature controller of the water bath is calibrated before the experiments.

In the consequent desorption step, nitrogen gas with a flowrate of 30 ml min^{-1} is conducted into the absorption cell with temperature set at 35 °C (45 °C in final step of desorption) to draw off the absorbed gas from the solution [3,7]. The endpoint of desorption process is determined by injection of the desorbed gas into the GC. In order to investigate the effect of temperature on desorption, further experiments are also made at different desorption temperatures.

The experiments are done at four temperatures of 5, 15, 25, and 35 °C. The time at which the first bubble exits from the absorption column is set as the start point of the experiment. The first sample is injected to the GC 1 min after beginning the experiment. Each injection takes 5 min to be completed. In order to track the absorption process precisely, consequent experiments are carried out with the same conditions, in which the injections are done with different time intervals. The endpoint of the experiment is determined when the outlet flowrate reaches to the influent flowrate.

4. Calculations

The momentary absorption of ethylene is defined as the mass of absorbed ethylene in unit volume of the absorbing solution at each time. It can be calculated by mass balance around the absorption column, i.e. the difference between the mass flowrates of the solute inlet to and outlet from the system:

$$\text{Momentary absorption of ethylene} = Q_{in}\rho_{in}x_{in} - Q_{out}\rho_{out}x_{out} \quad (1)$$

where $Q/cm^3\ min^{-1}$, $\rho/g\ cm^{-3}$ represent the volume flow rate and density of the gas mixture, respectively, and x is the mass fraction of ethylene. The subscripts of "in" and "out" denote to the inlet and outlet of the absorption column, respectively.

Gas density is calculated from the ideal gas law by knowing gas pressure and temperature, and the average molecular weight,

Table 1
Density and viscosity of ionic liquid with dissolved $AgNO_3$.

Material	Density ($g\ cm^{-3}$)				Viscosity (cP)			
	Temperature (°C)				Temperature (°C)			
	10	15	25	35	10	15	25	35
Pure IL	1.166	1.163	1.157	1.150	450.4	312.0	165.3	97.5
1 M $AgNO_3$ in IL	1.286	1.282	1.275	1.268	509.7	344.3	178.2	102.5
2 M $AgNO_3$ in IL	1.390	1.386	1.378	1.371	566.9	377.9	190.3	107.6
3 M $AgNO_3$ in IL	1.476	1.472	1.463	1.455	631.3	415.1	204.3	114.4
4 M $AgNO_3$ in IL	1.541	1.536	1.528	1.519	699.8	455.1	220.2	121.9
5 M $AgNO_3$ in IL	1.626	1.622	1.613	1.604	841.3	533.5	250.8	136.0
NMP	1.042	1.037	1.031	1.018	2.2	2.0	1.7	1.4
1 M $AgNO_3$ in IL:NMP (1:1 (vol.))	1.227	1.223	1.214	n.a.	29.9	24.0	16.4	n.a.
5 M $AgNO_3$ in IL:NMP (1:1 (vol.))	1.654	1.650	1.640	1.632	417.1	272.3	128.1	68.1

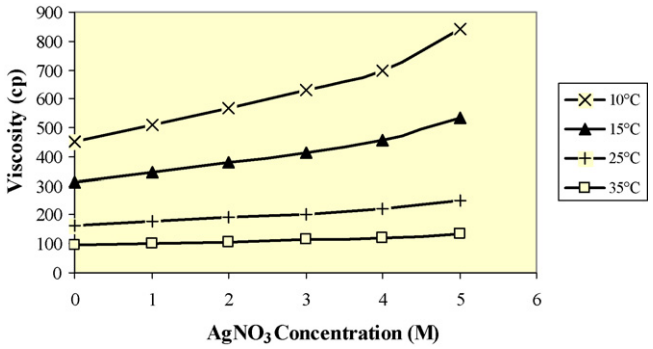

Fig. 2. Effect of $AgNO_3$ concentration in $[Bmim]NO_3$ on viscosity.

which is calculated based on the mole fraction of each gas. The densities calculated by the ideal gas law show negligible difference (about 0.6%) with those calculated by using the virial equation.

Integrating Eq. (1) by numerical methods over the time of experiment gives the total absorption of ethylene:

$$\text{Total absorption} = \left[\int_0^t (Q_{in}\rho_{in}x_{in} - Q_{out}\rho_{out}x_{out})\, dt\right] \quad (2)$$

5. Results and discussion

5.1. Effect of concentration on total absorption

5.1.1. Physical properties of reactive media

Since the density and viscosity of reactive media has an inverse effect on gas diffusion through the absorbing solution [25], the viscosities and densities of pure ionic liquid and its solutions with $AgNO_3$ are measured and reported in Table 1. The viscosities of solutions with different concentrations of $AgNO_3$ (1–5 M) are also shown in Fig. 2. The results show that as the temperature increases the viscosity decreases. In addition, viscosity is increased by increasing concentration of $AgNO_3$.

From the values of Table 1, it can be found that the viscosities of $AgNO_3$ solutions are significantly higher compared to the viscosities of aqueous solutions. Since the absorption is decreased as the viscosity is increased, in order to decrease viscosity of the solution, N-methyl pyrrolidone (NMP), which is a polar solvent with low vapor pressure and low viscosity, was added to ionic liquid with a 1:1 (vol.) ratio to produce 1 and 5 M of $AgNO_3$ solutions. As seen in Table 1, the viscosity of $AgNO_3$ solution in IL/NMP is lower than that for the solution of $AgNO_3$ in IL. The decrease in viscosity is especially significant for the 1 M solutions.

5.1.2. Total absorption

The total amounts of ethylene absorption for 1, 2 and 5 M silver nitrate concentrations are reported in Table 2 at 25 °C in two forms: the total amount of gas absorbed per solution volume (absolute absorptivity) in $g\,l^{-1}$, and moles of gas absorbed per moles of silver ion (molar absorptivity). This table shows that as the concentration of $AgNO_3$ is increased from 1 to 5 M, the absolute absorptivity is increased almost linearly. However, the molar absorptivity of the solution is increased moderately and then decreased. These results are in agreement with the findings of other researchers [12,26]. This behavior results from enhanced Ag^+/NO_3^- interactions in the concentrated solutions. These self-complexing interactions restrict the formation of the silver-olefin complex [12], which means lower degree of dissociation of silver nitrate in the concentrated solutions [11,27].

The molar absorptivity in the present research may be compared with the results of Sanchez et al. [28]. In their study, the molar absorptivity of ethylene in $[Bmim]NO_3$ with 2 and 4 M $AgNO_3$ at 60 °C were 0.044 and 0.019 $mol\,mol^{-1}\,Ag^+$, respectively, while in the present work, this value is 0.044 $mol\,mol^{-1}\,Ag^+$ in 2 M solution at 25 °C. The difference may be attributed to the difference of the applied setups and operational conditions.

In order to compare the effect of viscosity on absolute absorptivity, experimental results for gas absorption in 1 and 5 M solutions, with and without NMP, at different temperatures are reported in Table 3. As expected, absolute absorptivity of ethylene in 1 M solution with NMP is about 1.8–2.8 times higher than the value for solution without NMP at 25 and 5 °C, respectively. Also, the absolute absorptivities of ethylene at 5, 25 and 35 °C in 5 M solution with NMP are 5, 7 and 38% higher than those in 5 M solution without NMP.

The lower difference between the total absorptions in the solutions of 5 M $AgNO_3$ in IL and IL/NMP can be explained as follows: The degree of dissociation of Ag ions decreases as the concentration increases [27]. On the other hand, the degree of dissociation depends directly on the viscosity of the solution [29]. As seen in Table 1, at a specific temperature, the viscosity of 1 M $AgNO_3$ solution in IL/NMP is significantly lower than that for the solution of 1 M $AgNO_3$ in IL. On the other hand, although the viscosity of 5 M solution in IL/NMP is about half of the viscosity of 5 M $AgNO_3$ solution in IL, it is still considerably high. Therefore, as seen in Table 3, the absorption of ethylene for 1 M $AgNO_3$ solution in IL/NMP is much more than that "without NMP". On the other hand, the difference of absorptions for 5 M $AgNO_3$ solution in IL/NMP and for 5 M $AgNO_3$ solution in IL is not significant. In other words, the effects of concentration and viscosity on dissociation of Ag species are co-directional in this case. These effects may become more pronounced when the effect of viscosity on the gas diffusion in the liquid is also considered [25].

5.2. Effect of temperature on absorption

Temperature affects the absorption in a bilateral way where it causes decrease in viscosity and enhancing the ions mobility leading to increase in absorption, and on the other hand the solubility of ethylene (physical absorption) and also the rate of exothermic complexation reaction are decreased by increasing temperature [11,27]. Therefore, due to these mutual effects, it is expected that the absorption is attained to its maximum value within the range of temperature variation (5–35 °C). This is in agreement with our

Table 2
Total absorption of ethylene in absorptive solution at 25 °C.

$AgNO_3$ concentration/M	Total absorption of ethylene	
	$g\,l^{-1}$	$mol\,mol^{-1}\,Ag^+$
1	1.12	0.040
2	2.44	0.044
5	5.68	0.041

Table 3
Comparison between absolute absorptivities of 1 and 5 M solutions, without and with NMP.

$AgNO_3$ concentration/M	Temperature/°C	Total absorption of ethylene (g ethylene l^{-1})	
		Without NMP	With NMP
1	5	0.66	1.84
	25	1.12	2.04
5	5	4.92	5.18
	15	6.81	n.a.
	25	5.68	6.06
	35	4.83	6.68

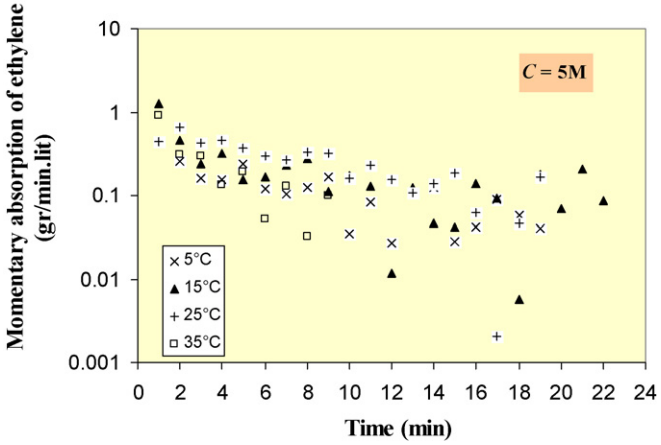

Fig. 3. Momentary absorption of ethylene in solution of $AgNO_3$ in $[Bmim]NO_3$.

observation as previously shown in Table 3, in which the maximum absolute absorptivity of ethylene is observed at intermediate temperatures of 15 and 25 °C.

In order to investigate the effect of temperature on absorption, the variation of momentary absorption in the solution of 5 M $AgNO_3$, which has the highest absorption, is shown in Fig. 3. Momentary absorption at initial times is in its maximum and strongly depends to temperature. The absorption is then decreased while at higher temperatures, due to lower equilibrium constant for complexation reaction, the decrement is faster [27].

The momentary absorptions for initial and intermediate times at different temperatures are shown in Fig. 4. As seen in the figure, momentary absorption for both times first increase by increasing temperature and reach to their maximums at 25 °C and decrease afterward. Difference in momentary absorption by altering temperature is larger at the initial time rather than at the intermediate time. In other words, the effect of temperature on absorption is more significant at initial times.

The time required for absorption to be completed, i.e. absorption time, for the solution of 5 M $AgNO_3$ at different temperatures is brought in Table 4. As seen in the table, the absorption time is shortened by increasing temperature from 5 to 35 °C for the solution without NMP, and from 15 to 35 °C for the solution with NMP. This is attributed to increase in the kinetic rate constant of the complexation reaction and its faster saturation at the higher temperatures.

Fig. 5 shows the momentary values of desorbed ethylene during desorption step. Large variation of momentary desorbed ethylene is observed at earlier times. However, it decreases along the time and approaches to zero after a relatively long time. Some differences are observed in the first 20 min due to differences in total absorption at different temperatures. The desorbed ethylene, which is corresponded to absorption temperature of 15 °C, is higher than that in the other temperatures.

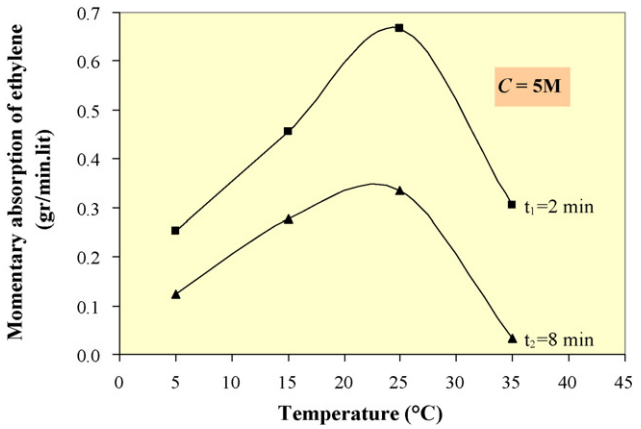

Fig. 4. Variation of momentary absorption of ethylene in solution of $AgNO_3$ in $[Bmim]NO_3$.

Table 4
Absorption time for 5 M solution of $AgNO_3$ in $[Bmim]NO_3$ without and with NMP.

Temperature/°C	Endpoint time/min	
	Without NMP	With NMP
5	31	20
15	29	23
25	27.5	20
35	26	10

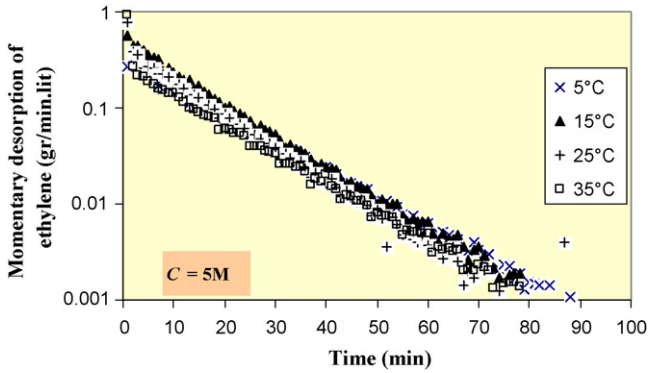

Fig. 5. Momentary desorption of ethylene corresponded to different absorption temperatures.

The momentary values of desorbed ethane during desorption step, which are corresponded to different absorption temperatures, are shown in Fig. 6. It is noticeable that all desorption processes were made at constant temperature of 45 °C. The amount of ethane is only considerable within the initial 2 min of desorption.

The same result can be found from Fig. 7, which shows the weight percent of ethane in the ethylene/ethane mixture in the outlet during desorption step. It is also noticeable that desorption of ethane in all of the experiments is lasted within about 20 min, and pure ethylene is desorbed from the system during desorption step after complete discharge of ethane. The amount of desorbed ethylene after complete discharge of ethane corresponded to the absorption temperatures of 5, 15, 25, and 35 °C is 1.026, 1.985, 1.247, and 0.939 g l^{-1}, respectively. These values are 21, 29, 22, and 19% of the total absorbed ethylene at those temperatures, respectively.

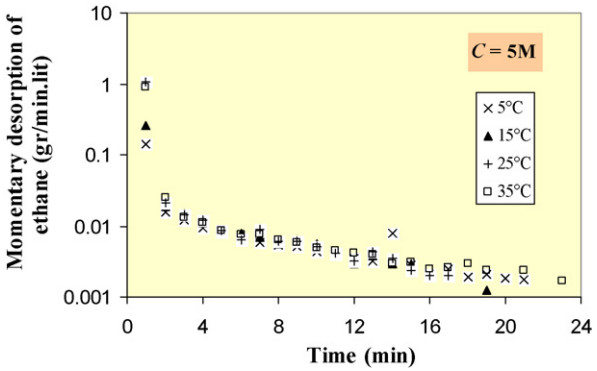

Fig. 6. Momentary desorption of ethane corresponded to different absorption temperatures.

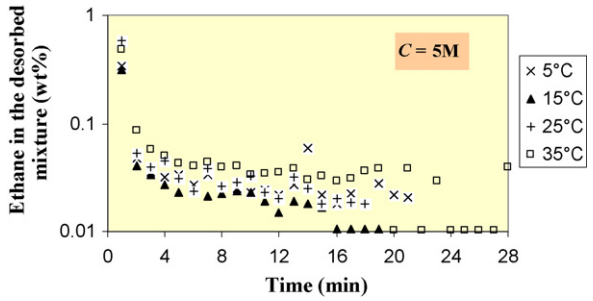

Fig. 7. Concentration of ethane in the desorbed mixture of ethylene/ethane.

Table 5a
Selectivity of ethylene to ethane in different concentrations at 25 °C.

$AgNO_3$ concentration/M	g C_2H_4 g^{-1} C_2H_6
1	1.30
2	1.84
5	3.36

Table 5b
Selectivity of ethylene to ethane at different temperatures in 5 M solution.

Temperature/°C	g C_2H_4 g^{-1} C_2H_6
5	15.38
15	13.90
25	3.36
35	3.29

5.3. Ethylene to ethane selectivity

The selectivities of ethylene to ethane in different concentrations at 25 °C are reported in Table 5a. The selectivities in 5 M solution at different temperatures are also reported in Table 5b. As seen in Table 5a, the selectivity is increased as the concentration of $AgNO_3$ is increased. This is because of more available Ag ions for complexation reaction with ethylene in the higher concentrations as also observed by Sanchez et al. [28]. On the other hand, the data in Table 5b shows that the selectivities at lower temperatures are significantly higher than those at higher temperatures. The decreasing trend of selectivity by increasing temperature is rather due to increasing in ethane absorption than decreasing in ethylene absorption. The increase in ethane absorption at higher temperature can be explained by considering the penetration model. This model predicts that in the absence of chemical absorption, the rate of physical absorption is proportional to the square root of gas diffusivity [30]. On the other hand, gas diffusivity is inversely in proportion to the liquid viscosity ($D \propto \mu_{IL}^{-0.66}$) [25]. As a result, ethane absorption is increased with decrease in viscosity at the higher temperatures.

6. Theoretical model for absorption

A theoretical model can be applied to predict the absorption of ethylene in the IL solution with $AgNO_3$.

The absorption flux in a chemical absorption process is enhanced by chemical reaction. It can be expressed as [31,32]:

$$N_A = \frac{1}{(1/E_A k_L) + (RT/Hk_g)}(C_A^* - C_{A,b}) \quad (3)$$

where N_A/mol cm^{-2} s^{-1} is the absorption flux of ethylene, C_A^*/mol cm^{-3} and $C_{A,b}$/mol cm^{-3} are the ethylene solubility and concentration of dissolved ethylene in the bulk liquid phase, respectively. E_A is the dimensionless enhancement factor, k_L and k_g/cm s^{-1} are liquid-side and gas-side mass transfer coefficients, respectively. R is the universal gas constant (8.314 J mol^{-1} K^{-1}), T/K absolute temperature, and H/bar cm^3 mol^{-1} is the Henry constant.

Mass transfer and associated reactions can be modeled in terms of the two-film theory with the following assumptions:

1. The reaction is assumed to be fast and of pseudo-first-order, and is carried out within the film. For this fast absorption regime, dimensionless Hatta number (Ha) is defined as [22]

$$Ha = \frac{\sqrt{k_{ov} D_A}}{k_L} \quad (4)$$

where k_{ov}/s^{-1} is the overall reaction rate constant and D_A/cm^2 s^{-1} is the diffusivity of ethylene in the solution. If the general reaction between solute ethylene (A) and a solution of Ag^+ (B) can be described as [27]

$$A(sol'n) + B(sol'n) \leftrightarrow A - B(sol'n) \quad (5)$$

forward reaction is assumed to be faster than the reverse reaction. Then, k_{ov} is obtained as follows [33]:

$$k_{ov} = \frac{-r_A}{C_A} = kC_B^{bulk} \quad (6)$$

where r/mol m^{-3} s^{-1} and k/m^3 mol^{-1} s^{-1} are the reaction rate and rate constant for the reaction between ethylene and Ag^+ ions, respectively. C_A/mol m^{-3} is the ethylene concentration. C_B^{bulk}/mol m^{-3} is the silver nitrate concentration in the bulk liquid phase. The order of magnitude for kinetic constant of complexation reaction is available in literature ($\sim 2 \times 10^2$ m^3 mol^{-1} s^{-1}) [27].
2. The gas-side mass transfer resistance is neglected ($1/k_g \cong 0$) [27].
3. Henry's law can be applied to estimate the solubility of gas in the ionic liquid.
4. The concentration of dissolved ethylene in the bulk liquid phase is assumed to be negligible for the entire reaction period ($C_{A,b} \cong 0$).
5. Gas volumetric flow rate is assumed to be constant.

By applying the enhancement factor based on the surface renewal theory [34]:

$$E_A = \sqrt{1 + Ha^2} \quad (7)$$

the rate of ethylene absorption can be calculated by combining Eqs. (3) and (4):

$$N = \frac{C_A^* a}{1/\left(k_L\sqrt{1 + (k_{ov}D_A/k_L^2)}\right)} = C_A^* a\sqrt{D_A k C_B^{bulk} + k_L^2} \quad (8)$$

where N/mol cm^{-3} s^{-1} (=$N_A \times a$) is absorption rate of ethylene and a/cm^{-1} is the interfacial area. C_A^* can be determined from Henry's law:

$$C_A^* = \frac{P_A}{H_A} \quad (9)$$

in which, Henry's constants for ethylene are available in literature [35]. P_A/bar is ethylene partial pressure.

The interfacial area is calculated from the observed hold-up in the experiments:

$$a = \frac{6\varepsilon}{d(1-\varepsilon)} \quad (10a)$$

$$\varepsilon = \frac{h - h_0}{h} \quad (10b)$$

where ε is the gas hold-up, d/cm is the bubble diameter, and h_0 and h/cm are the liquid level in absorption column before and after bubbling, respectively.

Table 6
Comparison of absorption rates obtained from theoretical model and experimental results.

Temperature/°C	$N_{Exp}/\times10^6$ mol cm^{-3} s^{-1}	$N_{Theo}/\times10^6$ mol cm^{-3} s^{-1}	$(\lvert N_{theo}-N_{exp}\rvert/N_{theo})$
5	0.179	0.190	0.058
15	0.195	0.263	0.259
25	0.219	0.255	0.141
35	0.378	0.258	0.465

The bubble diameter is determined by taking photos of the rising bubbles in the column. The bubbles in the present work have an ellipsoid shape for the viscous absorbing solution. It was observed that as the viscosity of the solution is decreased, the bubbles turn to a parabolic, and then to a spherical shape. The equivalent diameter of the bubbles is then calculated from [36]:

$$d = \sqrt[3]{F^2 \cdot f} \quad \text{(for ellipsoid)};$$

$$d = \sqrt[3]{\frac{3}{4} d_{pa}^2 \cdot h_{pa}} \quad \text{(for parabola)} \tag{11}$$

where F and f/cm are major and minor axis of the projected ellipsoid bubbles, respectively, and d_{pa} and h_{pa}/cm are the diameter and height of parabola-shaped bubbles, respectively.

Gas diffusivity can be calculated by the following Eq. [25]:

$$D_A = 2.66 \times 10^{-3} \frac{1}{\mu_{IL}^{0.66} v_A^{1.04}} \tag{12}$$

in which μ_{IL}/cP is the ionic liquid viscosity and v_A/l mol^{-1} is the gas molar volume at the normal boiling point determined using the method of Tyn and Calus [37].

Liquid-side mass transfer coefficient is determined using Higbie's penetration model:

$$k_L = \frac{2}{\sqrt{\pi}} \sqrt{\frac{D_A}{t_b}} \tag{13}$$

Time to traverse one bubble diameter, t_b/s, is calculated by using the observed rising bubble velocity and its diameter [38].

The experimental absorption rates were determined from the observed absorptions in 5 M $AgNO_3$ solution in IL and the absorption time. These observed values are compared with those obtained from the above theoretical model in Table 6. As seen in the table, there is a fairly good agreement between the theoretical model and the experimental results, which can verify the applied model. The calculated values of residual root mean square error (RMSE) and Chi-square test (χ^2) [39,40] are 0.010221 and 0.068402, respectively.

7. Comparison of total absorption in ionic liquid and in water with dissolved $AgNO_3$

Since aqueous $AgNO_3$ solution is often used for the absorption of ethylene from gaseous mixture, the values of total absorption in solutions of 5 M $AgNO_3$ in both ionic liquid and in water, obtained from the present system, are compared in Fig. 8. For comparison, the data obtained by Cho et al. [11] using aqueous $AgNO_3$ solution, are also shown in this figure (for supplementary data, see Table 7 [41,42]).

As seen in the figure, the absorption capacity of ionic liquid with dissolved $AgNO_3$ at 5 °C is about 0.17 of that for the aqueous solution in our study. This ratio at higher temperature of 25 °C is about 0.43. Therefore, applying ionic liquid with dissolved $AgNO_3$ at the higher temperature may be preferred.

A similar comparison was also carried out by Ortiz et al. for separation of propylene/propane using [Bmim]BF_4 + 0.25 M $AgBF_4$ at 25 °C. However, in contrary to our results, they found that the absorption of propylene in [Bmim]BF_4 is 1.2 times higher than that in 1 M aqueous media [18].

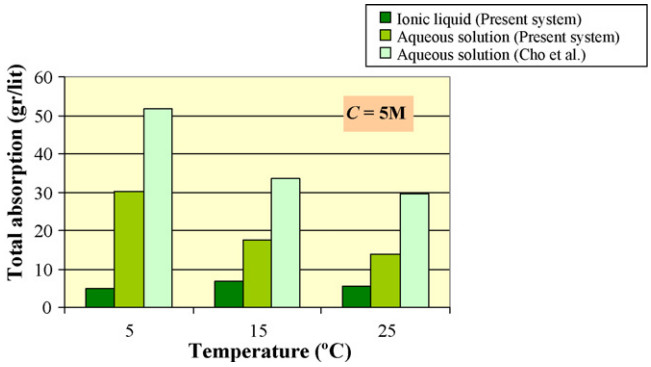

Fig. 8. Comparison of ethylene absorption for solutions of $AgNO_3$ in ionic liquid and in water.

Fig. 9 compares the absorption time in ionic liquid and in water solutions containing 5 M $AgNO_3$. As seen in the figure, except for 5 °C, in which absorption time for ionic liquid with dissolved $AgNO_3$ is about half of that for the aqueous solution, the absorption time for both solutions are almost the same at the other temperatures.

8. Solvent regeneration

The established bonds in chemical complexation are strong enough to achieve high selectivity and high capacity for the component to be bound. At the same time, the bonds are still weak so that they can be broken by using operations such as rising temperature or decreasing pressure [43].

Table 7
Experimental results of ethylene absorption in aqueous $AgNO_3$ solutions from present system compared to literature data.

Ref.	$[Ag^+]$/M	Temperature/°C	mol C_2H_4 mol^{-1} Ag^+
Present system [41]	1	5	0.39
		15	0.25
		25	0.18
	5	5	0.22
		15	0.12
		25	0.098
Crookes et al. [42]	0.1	20	0.39
	0.5		0.36
	1		0.35
	3		0.28
	5		0.22
	7		0.19
	9		0.17
Cho et al. [11]	1	5	0.55
		15	0.45
		25	0.18
	2	5	0.34
		15	0.29
		25	0.27
	5	5	0.37
		15	0.24
		25	0.21

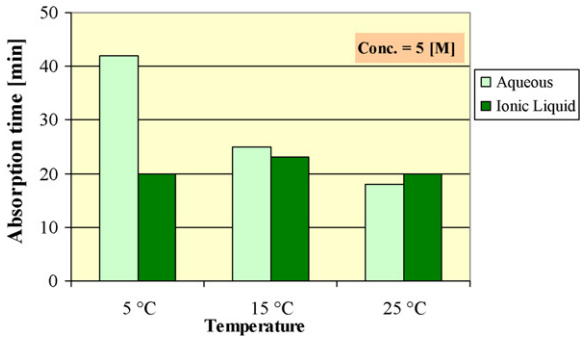

Fig. 9. Comparison of absorption time for aqueous and ionic liquid solutions of $AgNO_3$.

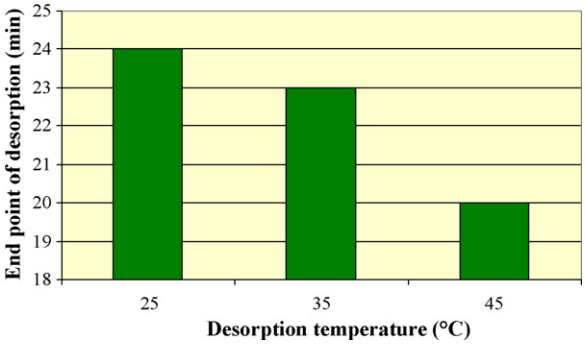

Fig. 10. Effect of temperature on desorption time from solution of 5 M $AgNO_3$ in $[Bmim]NO_3$.

In this study, a heated sweep gas was used to regenerate the solvent. The same separation efficiency of the repeated experiments indicates that a consistent regeneration was obtained and the silver–IL medium can be reused many times without any loss of absorption capability.

As mentioned earlier in Section 3, in order to investigate the effect of temperature on desorption, further experiments were made. In these experiments, the solution of 5 M $AgNO_3$ in IL was first saturated in the absorption column by ethylene at 20 °C, and the absorbed ethylene was then purged by nitrogen gas with a flowrate of 30 ml min^{-1} where different temperatures were set for the column in each run. As seen in Fig. 10, desorption time is shortened from 24 min to about 20 min when desorption temperature is increased from 25 to 45 °C. Although decreasing desorption time allows longer times for running the system in the absorption mode, i.e. the higher absorption capacity, it also increases the operational cost needed for heating up of the column. Therefore, the optimum desorption temperature and thus desorption period can be determined by a cost analysis, which considers the operational cost of desorption step against the fixed cost of the absorption column.

9. Conclusions

(1) Applying an appropriate ionic liquid ($[Bmim]NO_3$), which have the ability to dissolve $AgNO_3$ may solve the problems caused by the presence of vapor in the product when aqueous solution of $AgNO_3$ is used for the absorption of ethylene from the gaseous mixtures.
(2) The absolute absorptivity is increased almost linearly by increasing $AgNO_3$ concentration while the molar absorptivity of the solution is increased moderately and then decreased.
(3) High viscosity of $[Bmim]NO_3$ causes decrease in absorbing ability of the ionic liquid. Adding NMP as a low-viscosity solvent to the ionic liquid by a 1:1 volume ratio to produce 5 M $AgNO_3$ solutions could enhance absolute absorptivity by a factor of 5–38% when the absorption temperature is varied in the range of 5–35 °C.
(4) It is found that intermediate temperatures in the range of 15–25 °C are the optimum temperatures for absorption. This can be explained by considering bilateral effect of temperature, i.e. inherent decrease in gas absorption by increasing temperature due to decrease in solubility and reaction rate, and on the other hand enhance in the mass transfer flux due to decrease in viscosity by increasing temperature.
(5) The selectivity of ethylene to ethane is increased by increasing concentration while it is decreased by increasing temperature mainly due to higher absorption of ethane at high temperatures.
(6) The ethylene absorption capacity of the ionic liquid with dissolved $AgNO_3$ at 5 °C is about 0.17 of that for the aqueous $AgNO_3$ solution while this ratio is about 0.43 at 25 °C.

References

[1] C.L. Munson, L.C. Boudreau, M.S. Driver, W.L. Schinski, Process for the purification of olefins, US Patent, PCT/US01/17449, WO 01/98239, 2001.
[2] D.G. Bessarabov, R.D. Sanderson, E.P. Jacobs, High-efficiency separation of an ethylene/ethane mixture by a large-scale liquid-membrane contactor containing flat-sheet nonporous polymeric gas-separation membrane and a selective flowing-liquid absorbent, Ind. Eng. Chem. Res. 34 (1995) 1769–1778.
[3] K. Nymeijer, T. Visser, R. Assen, M. Wessling, Super selective membranes in gas–liquid membrane contactors for olefin/paraffin separation, J. Membr. Sci. 232 (2004) 107–114.
[4] R.B. Eldridge, Olefin/paraffin separation technology: a review, Ind. Eng. Chem. Res. 32 (1993) 2208–2212.
[5] Z. Lei, W. Arlt, P. Wasserscheid, Sepration of 1-hexene and *n*-hexane with ionic liquid, Fluid Phase Equilib. 241 (2006) 290–299.
[6] D.C. Nymeijer, T. Visser, R. Assen, M. Wessling, Composite hollow fiber gas–liquid membrane contactors for olefin/paraffin separation, Sep. Purif. Technol. 37 (2004) 209–220.
[7] D.T. Tsou, M.W. Blachman, Facilitated liquid membranes for olefin/paraffin gas separations and related processes, US Patent 5135547, 1992.
[8] I.H. Cho, H.K. Yasuda, T.R. Marrero, Solubility of propylene in aqueous silver nitrate, J. Chem. Eng. Data 40 (1995) 102–106.
[9] S. Duan, A. Ito, A. Ohkawa, Separation of propylene/propane mixture by supported liquid membrane triethylene glycol and a silver salt, J. Membr. Sci. 215 (2003) 53–60.
[10] J. Won, D.B. Kim, Y.S. Kang, D.K. Choi, H.S. Kim, C.K. Kim, C.K. Kim, An ab initio ionic liquid silver complexes as carriers in facilitated olefin transport membranes, J. Membr. Sci. 260 (2005) 37–44.
[11] I.H. Cho, H.K. Yasuda, T.R. Marrero, Solubility of ethylene in aqueous silver nitrate, J. Chem. Eng. Data 40 (1995) 107–111.
[12] D.J. Safarik, R.B. Eldridge, Olefin/paraffin separations by reactive absorption: a review, Ind. Eng. Chem. Res. 37 (1998) 2571–2581.
[13] K. Nymeijer, T. Visser, R. Assen, M. Wessling, Olefin-selective membranes in gas–liquid membrane contactors for olefin/paraffin separation, Ind. Eng. Chem. Res. 43 (2004) 720–727.
[14] N. Yamanouchi, S. Maetani, T. Aoki, A. Ito, VOC vapor permeation through triethylene glycol liquid membranes, in: 10th APPChE Congress, Japan, 2004.
[15] P. Husson-Borg, V. Majer, M.F. Costa Gomes, Solubilities of oxygen and carbon dioxide in butyl methyl imidazolium tetrafluoroborate as a function of temperature and at pressures close to atmospheric pressure, J. Chem. Eng. Data 48 (2003) 480–485.
[16] S.W. Kang, D.H. Lee, J.H. Park, K. Char, J.H. Kim, J. Won, Y.S. Kang, Effect of the polarity of silver nanoparticles induced by ionic liquids on facilitated transport for the separation of propylene/propane mixtures, J. Membr. Sci. 322 (2008) 281–285.
[17] S.W. Kang, J. Hong, K. Char, J.H. Kim, J. Kim, Y.S. Kang, Correlation between anions of ionic liquids and reduction of silver ions in facilitated olefin transport membranes, Desalination 233 (2008) 327–332.
[18] A. Ortiz, A. Ruiz, D. Gorri, I. Ortiz, Room temperature ionic liquid with silver salt as efficient reaction media for propylene/propane separation: absorption equilibrium, Sep. Purif. Technol. 63 (2008) 311–318.
[19] J.F. Huang, H. Luo, S. Dai, Advanced liquid membranes based on novel ionic liquids for selective separation of olefin/paraffin via olefin-facilitated transport, in: 2nd International Congress on Ionic Liquids (COIL-2), Yokohama, 2007.
[20] J.W. Chang, T.R. Marrero, H.K. Yasuda, Continuous process for propylene/propane separation by use of silver nitrate carrier and zirconia porous membrane, J. Membr. Sci. 205 (2002) 91–102.
[21] M. Teramoto, N. Takeuchi, T. Maki, H. Matsuyama, Ethylene/ethane separation by facilitated transport membrane accompanied by permeation of aqueous silver nitrate solution, Sep. Purif. Technol. 28 (2002) 117–124.
[22] M. Teramoto, S. Shimizu, H. Matsuyama, N. Matsumiy, Ethylene/ethane separation and concentration by hollow fiber facilitated transport membrane module with permeation of silver nitrate solution, Sep. Purif. Technol. 44 (2005) 19–29.

[23] J. Dupont, C.S. Consorti, P.A.Z. Suarez, R.F. De Souza, Preparation of 1-butyl-3-methyl imidazolium-based room temperature ionic liquids, Org. Synth. Coll. 10 (2004) 184.
[24] L. Cammarata, S.G. Kazarian, P.A. Salter, T. Welton, Molecular states of water in room temperature ionic liquids, Phys. Chem. Chem. Phys. 3 (2001) 5192–5200.
[25] D. Morgan, L. Ferguson, P. Scovazzo, Diffusivities of gases in room-temperature ionic liquids: data and correlations obtained using a lag-time technique, Ind. Eng. Chem. Res. 44 (2005) 4815–4823.
[26] B.B. Baker, The effect of metal fluoroborates on the absorption of ethylene by silver ion, Inorg. Chem. 3 (1964) 200–202.
[27] K. Nymeijer, T. Visser, W. Brilman, M. Wessling, Analysis of complexation reaction between Ag^+ and ethylene, Ind. Eng. Chem. Res. 43 (2004) 2627–2635.
[28] L.M. Galan Sanchez, G.W. Meindersma, A.B. De Haan, RTILs-based absorption solvents for olefin/paraffin separations, in: 2nd International Congress on Ionic Liquids (COIL-2), Yokohama, 2007.
[29] H. Weingartner, Corresponding states for electrolyte solutions, Pure Appl. Chem. 73 (2001) 1733–1748.
[30] R. Higbie, The rate of absorption of a pure gas into a still liquid during short periods of exposure, Trans. Am. Inst. Chem. Eng. 31 (1935) 365–389.
[31] A. Hartono, E.F. daSilva, H.F. Svendsen, Kinetics of carbon dioxide absorption in aqueous solution of diethylenetriamine (DETA), Chem. Eng. Sci. 64 (2009) 3205–3213.
[32] L.W. Lackey, R.O. Mines Jr., P.T. McCreanor, Ozonation of acid yellow 17 dye in a semi-batch bubble column, J. Hazard. Mater. B138 (2006) 357–362.
[33] A.F. Portugal, F.D. Magalhaes, A. Mendes, Carbon dioxide absorption kinetics in potassium threonate, Chem. Eng. Sci. 63 (2008) 3493–3503.
[34] J.A. Hogendoorn, R.D. Vas Bhat, J.A.M. Kuipers, W.P.M. Swaaij, G.F. Versteeg, Approximation for the enhancement factor applicable to reversible reactions of finite rate in chemically loaded solutions, Chem. Eng. Sci. 52 (1997) 4547–4559.
[35] J.L. Anthony, E.J. Maginn, J.F. Brennecke, Solubilities and thermodynamic properties of gases in the ionic liquid 1-n-butyl-3-methylimidazolium hexaflourophosphate, J. Phys. Chem. B106 (2002) 7315–7320.
[36] J.M. Navaza, D. Gomez-Diaz, M. Dolores La Rubia, Removal process of CO_2 using MDEA aqueous solutions in a bubble column reactor, Chem. Eng. J. 146 (2009) 184–188.
[37] B.E. Poling, J.M. Prausnitz, J.P. O'Connell, The Properties of Gases & Liquids, 5th ed., McGraw-Hill, 2001.
[38] M. Motarjemi, G.J. Jameson, Mass transfer from very small bubbles—the optimum bubble size for aeration, Chem. Eng. Sci. 33 (1978) 1415–1423.
[39] Y.S. Ho, W.T. Chiu, C.C. Wang, Regression analysis for the sorption isotherms of basic dyes on sugarcane dust, Bioresour. Technol. 96 (2005) 1285–1291.
[40] S.C. Tsai, K.W. Juang, Comparison of linear and non-linear forms of isotherm models for strontium sorption on a sodium bentonite, J. Radioanal. Nucl. Chem. 243 (2000) 741–746.
[41] H.R. Mortaheb, M. Mafi, A. Zolfaghari, B. Mokhtarani, N. Khodapanah, F. Ghaemaghami, Absorption of ethylene from ethylene–ethane gaseous mixture by agno3 solution in a semi-continuous process, Can. J. Chem. Eng. 87 (2009) 957–964.
[42] J.V. Crookes, A.A. Woolf, Competitive interactions in the complexing of ethylene with silver(I) salt solutions, J. Chem. Soc., Dalton Trans. 12 (1973) 1241–1247.
[43] C.J. King, Separation processes based on reversible chemical complexation, in: R.W. Rousseau (Ed.), Handbook of Separation Process Technology, Wiley, New York, 1987, pp. 760–774.